Modelling charge storage in Euclid CCD structures

Modelling charge storage in Euclid CCD structures

2012 JINST 7 C01058

(http://iopscience.iop.org/1748-0221/7/01/C01058)

Jinst

PUBLISHED BY IOP PUBLISHING FOR SISSA

RECEIVED: *October 26, 2011*
ACCEPTED: *December 19, 2011*
PUBLISHED: *January 13, 2012*

THE 9th INTERNATIONAL CONFERENCE ON POSITION SENSITIVE DETECTORS,
12–16 SEPTEMBER 2011,
ABERYSTWYTH, U.K.

Modelling charge storage in Euclid CCD structures

A.S. Clarke,[a,1] **D.J. Hall,**[b] **A. Holland**[a] **and D. Burt**[b]

[a] *e2v centre for electronic imaging,*
PSSRI, The Open University, England
[b] *e2v Technologies Plc,*
Chelmsford, England

E-mail: a.s.clarke@open.ac.uk

ABSTRACT: The primary aim of ESA's proposed Euclid mission is to observe the distribution of galaxies and galaxy clusters, enabling the mapping of the dark architecture of the universe [1]. This requires a high performance detector, designed to endure a harsh radiation environment.

The e2v CCD204 image sensor was redesigned for use on the Euclid mission [2]. The resulting e2v CCD273 has a narrower serial register electrode and transfer channel compared to its predecessor, causing a reduction in the size of charge packets stored, thus reducing the number of traps encountered by the signal electrons during charge transfer and improving the serial Charge Transfer Efficiency (CTE) under irradiation [3].

The proposed Euclid CCD has been modelled using the Silvaco TCAD software [4], to test preliminary calculations for the Full Well Capacity (FWC) and the channel potential of the device and provide indications of the volume occupied by varying signals. These results are essential for the realisation of the mission objectives and for radiation damage studies, with the aim of producing empirically derived formulae to approximate signal-volume characteristics in the devices. These formulae will be used in the radiation damage (charge trapping) models.

The Silvaco simulations have been tested against real devices to compare the experimental measurements to those predicted in the models. Using these results, the implications of this study on the Euclid mission can be investigated in more detail.

KEYWORDS: Detector modelling and simulations II (electric fields, charge transport, multiplication and induction, pulse formation, electron emission, etc); Solid state detectors

[1] Corresponding author.

doi:10.1088/1748-0221/7/01/C01058

2012 JINST 7 C01058

Contents

1 Introduction

The aim of the Euclid mission is to create detailed wide field images of the universe in order to calculate the weak lensing effect that dark energy masses will have on the light from distant galaxies. This will allow the mass of the intervening dark energy to be calculated without knowledge of its composition, to produce a dark energy map of the universe [5, 8].

The detector used on the proposed mission will be formed from an array of CCD273s [2]. These devices were designed and are currently being manufactured by e2v (U.K.). The detector was specifically designed for Euclid, based on an older device, but with changes designed to improve CTE under irradiation. The design changes were necessary due to the harsh operating environment (the estimated end-of-life 10 MeV proton fluence is around 6×10^9 protons cm^{-2} in the worst case, where the satellite orbit is at L2) and to provide the high accuracy required for a good weak lensing survey.

Radiation damage causes electron traps to form in solid state imaging devices. If the traps are located in the buried channel, these traps can capture electrons from passing charge packets during transfer. Traps with fast emission times may release the captured charge into an adjacent packet, distorting (or "smearing") the image PSF [6].

It is necessary to reduce the effects of radiation damage on the images captured such that distortion due to weak lensing can be separated from distortion caused by radiation damage. The aim of this work is to aid the calibration of the radiation damage models and also to aid in the post processing of images to remove the effects of radiation damage. The radiation damage models

require knowledge of electron distributions in the device structure such that the probability of trapping can be calculated more accurately.

This study details the electron distributions obtained from three-dimensional models of the Euclid device structures to calculate charge packet volume, produced using the commercially available Silvaco ATLAS software [4]. The aim is to enable the calibration of the radiation damage models through empirically derived formulae which approximate charge packet volume, based on the observations of the charge packet in the device simulations.

The device models are benchmarked using measurable parameters against values measured in test devices to ensure consistency. However, charge packet volume cannot be directly measured in the test devices and so it has to be inferred from CTE characterisation results. The change in CTE performance between the two devices (CCD273 and CCD204) is related to the volume occupied by charge packets and will indicate the general accuracy of the signal-volume models.

2 Radiation damage

Charge is read out of CCDs by transferring the charge stored in each pixel in parallel along the transfer channels until it reaches the register, and then transferred along the register in series until it reaches the readout node, where it is output from the device. These charge packets can undergo thousands of transfers until they reach the output node, depending on the size of the CCD and their starting location in it, so it is essential that the CTE is optimized to preserve image fidelity.

High energy particles incident on the detector cause displacement damage in the silicon lattice, where Si atoms in the path of the particle are pushed away from their lattice position leaving behind a vacancy. These vacancies are unstable and are able to migrate through the device until they become stable. Phosphorous atoms are able to stabilise these vacancies, but the combination of Si vacancy and P atom creates an electron trap known as a PV centre [7].

Phosphorus is the element used predominantly to dope the buried channel in n channel devices; as such PV centres are likely to be located randomly throughout the buried channel. Traps located in the buried channel will be able to trap charge from passing charge packets, thus reducing CTE.

2.1 Emission

Traps with emission times much larger than the readout speed, may release trapped charge after the image has been read out of the device, thus reducing the signal levels. Traps with shorter emission times, comparable to the transfer time from pixel to pixel, may release trapped charge from one charge packet into the next, distorting the PSF of a point source such as an astronomical object. This effect is critical in the Euclid mission where the weak lensing survey depends on the accurate measurement of distortion of galaxy shapes and positions [1].

2.2 Capture probability

The radiation damage models calculate the probability of capture using Shockley-Read-Hall theory [9]. The only traps affecting charge transfer are those in the vicinity of the charge packet, making the signal-volume models essential for a more realistic radiation damage model. The signal-volume plots are produced using the Silvaco models of the detector device structures with charge

2012 JINST 7 C01058

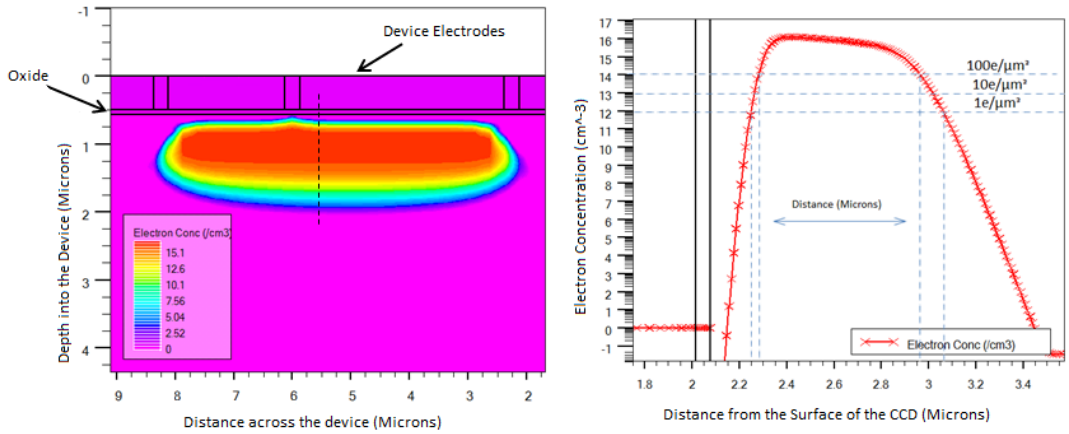

Figure 1. a) shows a 2D cross section of the charge packet in the Euclid pixel, b) is the 1D plot of electron concentration across the charge packet shown in a), indicated by the dashed line.

induced, allowing the observation of the charge packet size, location and density. Plotting the volume occupied by the charge packet against the signal size gives rise to functions which describe the signal-volume relation. It is these functions which are used in the radiation damage models.

2.3 Signal-volume in Silvaco Models

Images of the charge packet in 2 dimensions can be taken from the 3D device models, as in figure 1a. The charge packets have a high density core, equivalent to the maximum doping density for the buried channel. This reduces gradually at the edges of the charge packet until it becomes negligible. A 1D plot of charge density can be taken across the charge packet to measure its dimensions, figure 1b, which allows an approximation of the charge packet volume.

It is necessary to take different charge density cut off values to define the edge of the charge packet because of the gradually reducing edge density. These values effectively define the 'trapping volumes', as charge trapping is dependent on the charge density in the vicinity of a trap [9]. Therefore, areas where the charge density of the signal is sufficient for capture can be approximated by a function produced from the signal-volume model.

Each of the charge density cut off values used to define the edge of the charge packet are shown in figure 1b, 1 electron μm^{-3} is equivalent to 10^{12} electrons cm^{-3}, 10 electrons μm^{-3} is equivalent to 10^{13} electrons cm^{-3} and 100 electrons μm^{-3} is equivalent to 10^{14} electrons cm^{-3}. For reference, $\approx 10^{10}$ electrons cm^{-3} is the carrier concentration of intrinsic silicon.

2.4 Benchmarking

The models need to be verified and benchmarked to ensure they offer a realistic representation of the Euclid device. The aim of the models is to gain functions which describe the charge packet volume over a range of signal levels for use in the radiation damage studies. However, the volume values obtained cannot be directly verified, since charge packet volumes cannot be directly observed in the test devices.

2012 JINST 7 C01058

Table 1. Comparison of model values against preliminary test results.

	Silvaco Model	Experimental Results
	CCD273 Pixel	CCD273 Pixel
FWC (electrons)	180k - 240k	212k
Φ_{ch0} (Voltage)	6.9	7.1

Other measureable parameters such as channel potential (Φ_{ch0}) and Full Well Capacity (FWC) are taken to give a good indication of the model's general accuracy. Verifying the signal-volume model is more difficult but can be done through CTE characterisation, where a change in CTE performance between the CCD273 and the CCD204 can be compared against the change in charge packet volume in the models of the two devices. However, this only offers an indirect indication of the model accuracy and is dependent on several assumptions for trap interaction. Further verification will come from the effectiveness of the radiation damage models to which this work contributes [9].

The FWC is a soft parameter because its value can vary depending on the limits set, due to the fringing fields and measurement method, so a value range is given. The experimental results are obtained from the first batch of manufactured devices shown in table 1.

The values in the table show a rough agreement between the Silvaco models and the first test devices. Benchmarking work is ongoing.

2.5 Signal-volume theory

Current trapping models make assumptions about charge packet volume to model the charge transfer in CCDs. The various models can be described by the interaction volume function given in an ESA technical note written by A. Short [11], shown in equation (2.1) and graphically in figure 2.

$$\frac{V_C}{V_g} = \left(\frac{N_e}{\mathrm{FWC}}\right)^{\beta} \tag{2.1}$$

Where V_C is the volume of the charge packet, V_g is the volume of the charge packet at full well capacity, N_e is the signal size, FWC is the signal size at full well capacity and β is simply a fitting parameter which describes how the charge packet changes with signal size.

One of three assumptions about the charge packet might be made [10]:

- A charge packet will always fill the volume available to it, only increasing its charge density when charge is added (density driven model, $\beta = 0$).
- Charge density will remain constant and only the volume which the charge packet occupies will increase as charge is added (volume driven model, $\beta = 1$).
- Alternatively, somewhere in between the two extremes, where both charge density and charge packet volume change as charge is added ($0 < \beta < 1$).

This final assumption is currently thought to be the most physically realistic overall, but there may be some deviation from the trend at small signal levels.

2012 JINST 7 C01058

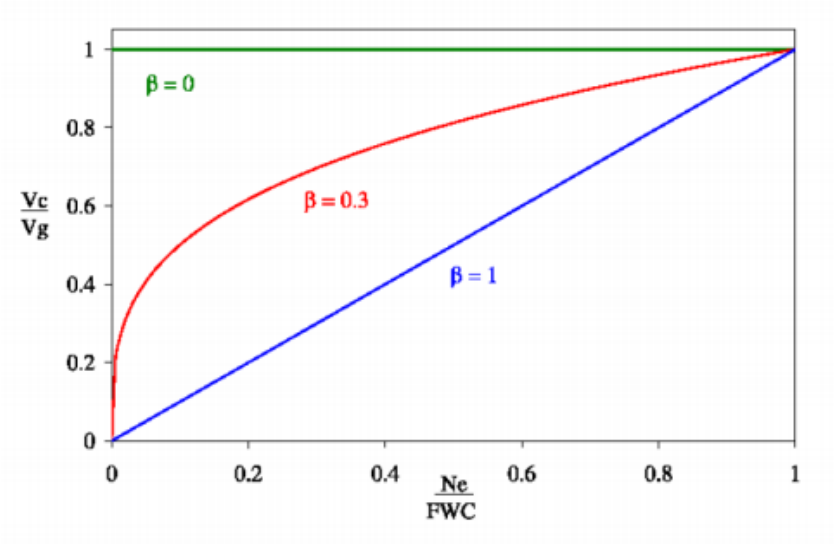

Figure 2. Plot of the signal-volume function [11], showing the density driven model ($\beta = 0$), volume driven model ($\beta = 1$) and the more realistic assumption ($0 < \beta < 1$), normalised against FWC.

It is possible to observe and measure the charge packets in the Silvaco device simulations in three dimensions, figure 1. These charge packets do not have a well defined edge, but gradually reduce in charge density until the density becomes negligible. When measuring the charge packet dimensions in the models it is necessary to take a cut off such that the charge packet can be measured and the volume calculated for each cut off density. In this way plots of volume against signal size can be produced, figure 3. Measurements of charge packet volume are used to derive an empirical formula for use in the radiation damage models to describe the changing volume with signal.

The volume calculations are static measurements, but Shockley-Read-Hall theory shows that the probability of capture is dependent on charge density in the vicinity of the trap, capture cross section (this varies for different traps) and dwell time of the charge packet under each CCD phase. The functions derived from the signal-volume plots can be related to the capture time constant, depending on the trap species and the charge density, to calculate capture probability in the radiation damage models for different dwell times which relate to the CCD clocking schemes [9].

3 Signal-volume characterisation.

The signal-volume plot produced, as shown in figure 3, gives the image area pixel (left) and readout register element (right) for the CCD273. It is worth noting that the theoretical plot in figure 2 is normalised against FWC and FWC volume, but the FWC of the two structures in figure 3 are different, hence the adjacent figures are plotted over a different range of signal sizes.

These signal-volume distributions are shown over a logarithmic scale but the plots follow a curve similar to that shown in figure 1, when the fitting parameter (β) lies between 0 and 1 (i.e. both charge density and volume change as charge is added to the packet).

The trapping volume diverges at small signal levels across the different cut off densities because the electrons which make up the charge packet disperse across the volume available in the

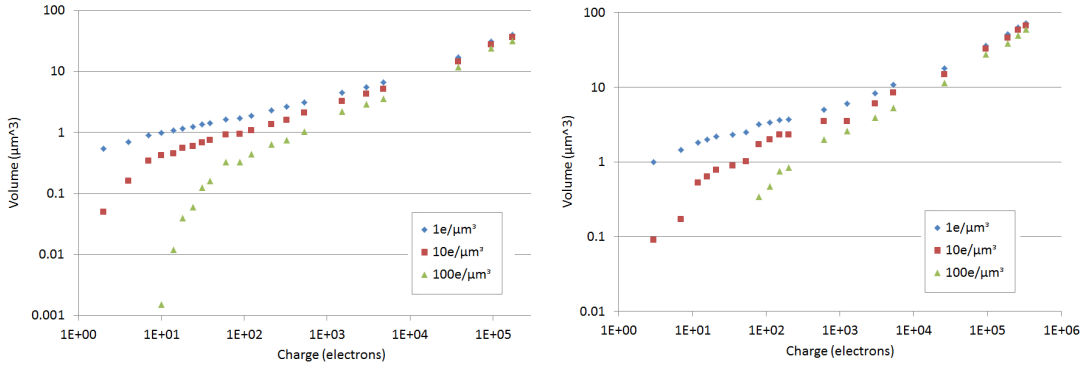

Figure 3. The signal-volume plots for a) the pixel and b) the readout register structures of the CCD273 in logarithmic scale.

device, reducing the overall charge density and making the low density volumes bigger. At larger signals, close to the FWC, the difference in trapping volumes across the cut off values becomes much less pronounced, as the charge packet becomes more densely populated across the whole available volume.

With very small signals (less than 100 electrons), the volume measurement for the cut off density defined as 100 electrons μm^{-3} (10^{14} electrons cm^{-3}) becomes less reliable due to the low signal level. The same error can be seen on the 10 electrons μm^{-3} plot when the signal level drops below 10 electrons. The values of the lower density cut off measurements are most reliable at these low signal levels.

At small signal the gradient of the signal-volume plot appears to flatten, before the small signal errors mentioned previously begin to appear. This changing gradient is not included in the simple volume function of equation (2.1), but might be expected according to some signal-volume models [10].

The generally linear trend of the plots in figure 3 at larger signals, gives rise to simple functions which can describe the increasing charge packet volume in relation to the signal size; this enables the charge trapping models to be as realistic as possible. However, the reducing gradient at small signals, as evident for 1 electron μm^{-3}, diverges from that predicted in theory so an extra variable is necessary in the signal-volume function.

4 Implications for charge transfer

The functions derived from the signal-volume plots are in the form:

$$\text{Volume} = \gamma S^{\beta} + \alpha \tag{4.1}$$

Where S is the signal size, β is the fitting parameter as already described, α describes the changing gradient at small signal and γ is a scaling factor which depends on the cut off density [9].

Using the different cut off densities to define the edges of the charge packet allows the separation of trap time constants according to SRH theory [9] and enables trapping volumes to be defined, where outside this volume the charge density is not high enough to trap electrons in the transfer

2012 JINST 7 C01058

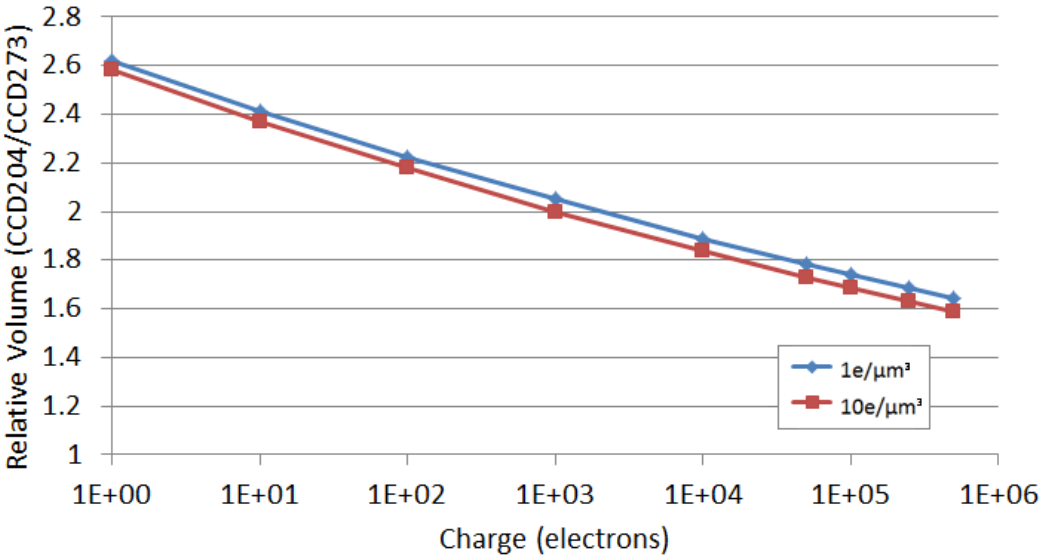

Figure 4. Ratio of the volumes occupied by varying charge packet sizes in the CCD204 readout register when compared to the CCD273 read out register.

period. Deriving the functions allows the charge trapping to be modelled as closely as possible to the physical system.

5 Comparison of the CCD273 vs. CCD204

The CCD273 is redesigned from the older CCD204 to improve operation under irradiation, which is achieved by reducing the width of the transfer channel in the serial readout register from 50 μm to 20 μm.

It is assumed that this 2.5 times reduction in channel width will improve serial CTE under irradiation by roughly the same factor, by reducing the volume in which the charge packets stored. After simulating the charge packet volume in both device structures and extracting the fitting parameters it is possible to plot a comparison of the volume occupied by the same charge packet across the two structures.

The difference in volume occupied in each device is shown in figure 4. The lower density cut off values are plotted to offer a more realistic impression of the volume difference between charge packets in the two devices as the high density area in the middle of the charge packet is not representative of the overall charge packet size.

The plot shows that the difference in the charge packet volume at small signals ($N_e < 1000$) is approximately 2.5 times larger in the CCD204, as expected. However as signal levels increase the difference in volume occupied between the devices reduces to a factor of around 1.5 at high signal levels. This will reduce the expected improvements of CTE at high signals and offers a way in which the devices can be tested to confirm the suitability of the models, by measuring the improvement in CTE between the devices over a signal range.

2012 JINST 7 C01058

6 Conclusion

The aim of these device models is to produce simple functions to approximate the interaction (trapping) volumes of charge packets in the CCD273 pixel and register structures. These functions will be used to help develop more realistic radiation damage models. The radiation damage models reproduce the effects which radiation damage has on images, with the aim of eventually post processing captured images to remove the effects of radiation damage. This information can only be approximated from device models as charge packets cannot be observed in test devices.

Device parameters such as FWC and the channel potential (Φ_{ch0}) closely match those measured in the first production batch of the CCD273, verifying the general accuracy of the model and giving confidence in the signal-volume models which cannot be directly confirmed. These generally follow the trend expected for increasing charge packet volume described by the interaction volume function [9]. However, the signal-volume plots deviate from the expected trend at smaller signals creating the need for an extra variable in the function.

At high signal levels ($N_e > 1 \times 10^4$ electrons), the difference in trapping volumes observed between the CCD273 and the CCD204 is significantly lower than the expected 2.5 times factor. This will limit the expected improvement in CTE in this signal range. However, at small signals the volume difference between charge packets in the two devices is approximately 2.5 times larger in the CCD204. This should allow the expected 2.5 times improvement in CTE performance in this signal range, where it is needed to meet the Euclid mission objectives. These findings will be verified during future CTE characterisation of the devices.

Acknowledgments

With thanks to the staff at The Open University and at e2v Technologies who have helped and contributed to this work.

References

[1] ESA, *Euclid Science Requirements*, DEM-SA-Dc-0001_1_0_Euclid_SciRD_2008, (2008).

[2] S. Bowring, e2v technologies plc. *CCD273 Design Report*, EUCV-E2V-RP-002, (2010).

[3] J. Pickel et al., *Radiation Effects on Photonic Imagers- A Historical Perspective*, *IEEE Trans. Nucl. Sci.* **50** (2003) 12.

[4] Silvaco Inc., *ATLAS User's Manual* (2010).

[5] R. Laureijs, *Euclid Science Requirements*, DEM-SA-Dc-00001, (2008).

[6] S.B. Howell, *Handbook of CCD Astronomy*, Cambridge University Press (2006), pp. 94–95.

[7] J.R. Srour et. al, *Review of Displacement Damage Effects in Silicon Devices*, *IEEE Trans. Nucl. Sci.* **50** (2003) 653.

[8] A. Refregier et. al, *Summary of DUNE Mission Concept*, *Proc. SPIE* **7010** (2008) 701018.

[9] D.J. Hall, *Euclid Monte Carlo Charge Transfer Model*, Open_Euclid_TR_09.01, (2010).

[10] D.J. Hall, *Comparison and Applicability to the Euclid Mission of the ESA CDM and the OU Monte Carlo modelling of CCD Radiation Damage*, OPEN_EUCLID_TR-20-V1, (2011).

[11] A. Short, *A Charge Distortion Model for Euclid*, EUCLID_TN_ESA_AS_003_0, (2010).

2012 JINST 7 C01058